RESEARCH PAPER

Adaptive identification of anaerobic digestion process for biogas production management systems

Kazuto Yoshida[1] · Keita Kametani[1] · Naoto Shimizu[2]

Abstract
To achieve the goals of sustainable development, supplies of renewable energy must be increased and methods of stable production developed. This study focused on the anaerobic digestion process using biomass as a raw material, which represents a renewable energy resource which is robust to environmental change and can be adjusted to suit supply and demand. A state-space model of the process was built in this study, consisting of two differential equations and one algebraic equation. The parameters included in the model are dependent on the operating conditions of the process. Automatic estimation of parameters from the input and output data of the process enables easy use of the model under any operating conditions. An adaptive-identifier control system was introduced as the parameter-estimation system, which made it possible to obtain the least squares estimate of parameters. When accumulated biogas generation per day was predicted using the model, goodness-of-fit analysis indicated an accuracy of over 80% in all cases, validating the model and estimated parameters. Future tasks will involve implementation of model predictive control into anaerobic digestion processes with the model and parameter-estimation system developed in this study.

Keywords Anaerobic digestion process · State-space model · Parameter estimation · Adaptive identification

Introduction

Presently, there is a strong worldwide reliance on non-renewable resources such as fossil fuels. The current situation, in which these resources are becoming scarce, means that the necessary cessation of all production activities is becoming a significant risk. Increasing and stabilizing the supply of renewable energy, which will not be exhausted, are key in the achievement of sustainable-development goals. However, the production of renewable energy by wind and solar power, which currently represent the largest contribution to renewable energy worldwide, fluctuates according to environmental conditions. These resources are therefore termed variable renewable energy sources. Stable power sources such as thermal or nuclear power and energy carriers

such as hydrogen must be produced by advanced technology to compensate for the output fluctuation of renewable energy, and enable its practical use. Biomass is a renewable resource that is robust to environmental changes. This has attracted a lot of interest because it represents a raw material from which an energy system can be developed that is completely independent of fossil fuels. Such a system, involving the combination of variable renewable energy and robust energy, can compensate for fluctuations in the output of variable renewable energy sources through the production of energy from biomass. The issue of biogas production should be managed so that the energy supply is stabilized.

Of the energy production technologies that utilize biomass, anaerobic digestion is an excellent method, which can simultaneously perform waste treatment and energy recovery [1, 2]. Furthermore; the digestate, which is a by-product of anaerobic digestion, can be used as a fertilizer [1, 2]. The numerical optimization of the anaerobic digestion process has been studied for various methods. Mendez-Acosta et al. regulated volatile fatty acid concentration and total alkalinity, inhibitors of anaerobic digestion, to improve process stability using a dynamic model [3]. Mauky et al. developed a feeding management strategy to compensate

✉ Naoto Shimizu
shimizu@bpe.agr.hokudai.ac.jp

[1] Graduate School of Agriculture, Hokkaido University, Sapporo, Hokkaido 060-8589, Japan

[2] Agricultural Engineering Laboratory, Research Faculty of Agriculture, Hokkaido University, Kita 9 Nishi 9, Kita-ku, Sapporo, Hokkaido 060-8589, Japan

for the difference between energy supply and demand in the International Water Association (IWA) Anaerobic Digestion Model No. 1 (ADM1) [4, 5]. Therefore, there have been some attempts to exploit the advantages of anaerobic digestion for energy supply and demand adjustments, and the models enable accurate prediction of gas generation and offer flexibility and robustness in various operating conditions. However; in terms of feasibility, the construction of a model for control of biogas production is complex because the current biogas generation prediction model has many parameters which must be determined in the various different operating conditions (for example, the temperature of the digester and solid concentration of the sludge) [6]. It is cumbersome and undesirable to determine all of the parameters included in ADM1 for each operating condition experientially. A simplified model for the prediction of biogas generation may address some of these challenges. From the viewpoint of feasibility at the industrial scale of a biogas plant, Hend et al. developed a simple model of biogas generation and conducted a parametric study for optimization of the model constants [7].

It is not possible to compensate for fluctuations in the output of variable renewable energy because the process is currently used for treating daily waste (e.g., food waste), and the amount of raw material input is therefore limited. If the raw material input is changed rapidly, the fermentation state may shift excessively and inhibit fermentation [8]. An improved model for predicting biogas generation while presuming the fermentation state is needed. To this end, AMD1 is widely used, but the present study aimed to represent the state-space of the anaerobic digestion process due to the above-mentioned reasons. The state-space model can predict the unobserved fermentation state, including parameters such as bacterial and substrate concentrations, from the measured gas flow rate. Furthermore, it is preferable to be able to easily estimate the parameters contained in the model. The objective of this study was, therefore, to construct a state-space model that is suitable for controlling biogas production as well as a system that can automatically estimate the necessary parameters representing input and output characteristics of the anaerobic digestion process from actual operation data.

Materials and methods

Anaerobic digestion process flow

Figure 1 presents the flow diagram of the anaerobic digestion process used in this study. Food waste from the cafeteria and copy-paper waste from Hokkaido University were used as raw materials. Food waste was ground using a food processor and copy-paper waste was cut using a shredder. Food waste was bagged in small portions and stored frozen, and paper waste was stored at ambient temperature until use as feedstock. To make the feedstock, N-rich material—namely, food waste—was mixed with paper as an auxiliary material to adjust the C/N ratio to around 40 to reduce ammonia inhibition (which
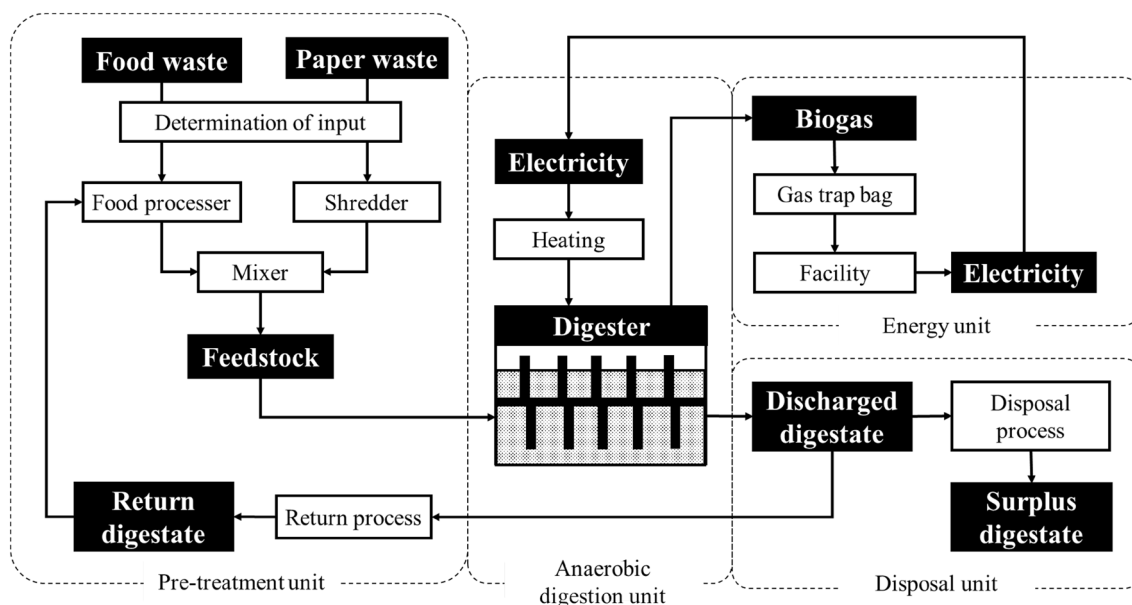
Fig. 1 Anaerobic digestion processing flow. Feedstock prepared in the pre-treatment unit from food and paper waste was added to the anaerobic digester in an anaerobic-digestion unit. Biogas was col-lected by gas trap bag in the energy unit and the digestate was disposed of via the disposal unit

can be a result of anaerobic digestion of N-rich feedstock) [9, 10]. To this end, the ground food waste and shredded paper were mixed in a mass ratio of 2.5:1. The resulting feedstock was added to a horizontal cylindrical reactor (effective volume: 0.235 m³) which was heated to around 52 °C and regularly stirred to allow for degassing and ensure adequate mixing of the feedstock. Biogas was collected using a gas trap bag. A portion of the discharged digestate was collected at the time of feeding and the residual digestate (excluding the returned digestate) was taken as the surplus digestate.

The total and volatile solids contents of the feedstock were about 40% and 35%, respectively. The sludge in the reactor was maintained at thermophilic temperature (52 °C). The anaerobic digestion process flow that was used in this study was therefore classified as dry thermophilic processing, and was expected to minimize digestate emissions because additional water was not required [6].

State-space model of anaerobic digestion process

We made some assumptions about the anaerobic digestion process to simplify the construction of the model. The overall reaction from the input of organic compounds (substrate) to biogas generation is represented by the model. The reactor was a semi-batch type and its sludge flow was complete-mixing flow. The volume of sludge in the reactor remained constant at 0.200 m³. To describe the mathematical state of the process, the bacterial concentration "$n(t)$" and substrate concentration "$s(t)$" were considered as the state variables that represented the fermentation status of the reactor. The bacterial and substrate concentrations in the feedstock were considered the manipulated variables "$u_n(t)$" and "$u_s(t)$", respectively, and biogas was a controlled variable "$v(t)$". Using these factors, the reactor was simplified as shown in Fig. 2.

The mathematical model of anaerobic digestion was based on the mass balance theory. The state equation comprises two differential equations; the first representing bacterial growth and the second representing substrate decomposition. In this study, we used the logistic difference equation to represent bacterial growth, as it is an effective equation in the field of population biology [7]. The substrate decomposition equation shows that degradation of the substrate occurs in line with bacterial growth. The output equation refers to biogas flow rate, which represents the generation of biogas as the substrate decomposes and the bacteria multiply [11]. The specific growth rate in these equations is given by the modified Monod
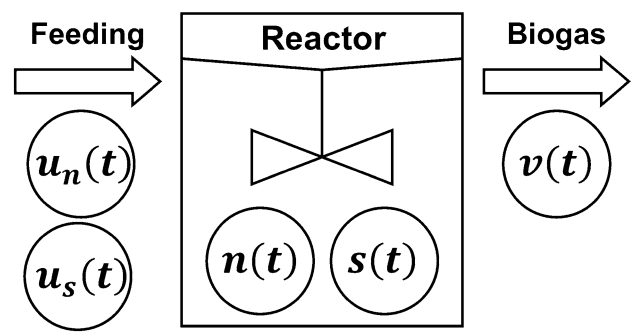
Fig. 2 Graphical representation of the semi-batch-type reactor used for anaerobic digestion in the present study. $u_n(t)$ bacterial input (kg/m³/h), $u_s(t)$ substrate input (kg/m³/h), $n(t)$ bacterial concentration (kg/m³), $s(t)$ substrate concentration (kg/m³), $v(t)$ biogas flow rate (m³/h)

equation [12]. The mathematical model of the anaerobic digestion process is given by concatenating two differential equations and one algebraic equation (Eq. 1):

$$\begin{cases} \frac{dn(t)}{dt} = (\mu(s) - b)n(t)\left(1 - \frac{n(t)}{n_{max}}\right) + u_n(t) \\ \frac{ds(t)}{dt} = -\frac{1}{Y}\mu(s)n(t) + u_s(t) \\ v(t) = \left(k_{g1}b + k_{g2}\frac{1}{Y}\mu(s)\right)mn(t) \end{cases}$$

$$\mu(s) = \mu_{max}\frac{s(t)}{k_s + s(t) + k_i s^2(t)}$$

$\qquad(1)$

where $n(t)$ is the bacterial concentration (kg/m³), $\mu(s)$ is the specific growth rate (h⁻¹), b is the autolysis rate (h⁻¹), n_{max} is the maximum bacterial concentration (kg/m³), $u_n(t)$ is the bacterial input (kg/m³/h), $s(t)$ is the substrate concentration (kg/m³), Y is the bacterial cell yield, $u_s(t)$ is the substrate input (kg/m³/h), $v(t)$ is the biogas flow rate (m³/h), m is the sludge volume (m³), k_{g1}, k_{g2} is the biogas generation coefficients, μ_{max} is the maximum specific growth rate (h⁻¹), k_s is the dissociation constant (kg/m³), and k_i is the inhibition coefficient.

The perturbation method near the equilibrium point was applied to this nonlinear model. By disregarding the second- and higher-order terms after Taylor expansion of a two-variable function, referring to the appendix for details (Eq. 8–11), the linear time invariant state-space model was obtained (Eq. 2):

$$\frac{dX(t)}{dt} = A_p X(t) + B_p U(t)$$

$$y(t) = C_p X(t),$$

where: $X(t) = \begin{bmatrix} n(t) \\ s(t) \end{bmatrix}, \quad U(t) = \begin{bmatrix} u_n(t) \\ u_s(t) \end{bmatrix}, \quad y(t) = v(t),$

$$A_p = \left. \frac{\partial F}{\partial X(t)} \right|_{(X_{eq}, U_{eq}, t)} = \begin{bmatrix} a_{11} & a_{12} \\ a_{21} & a_{22} \end{bmatrix},$$

$$B_p = \left. \frac{\partial F}{\partial U(t)} \right|_{(X_{eq}, U_{eq}, t)} = \begin{bmatrix} b_{11} & b_{12} \\ b_{21} & b_{22} \end{bmatrix},$$

$$C_p = \left. \frac{\partial g}{\partial X(t)} \right|_{(X_{eq}, t)} = \begin{bmatrix} c_{11} & c_{12} \end{bmatrix},$$

$a_{11}, a_{12}, a_{21}, a_{22}, b_{11}, b_{12}, b_{21}, b_{22}, c_{11}, c_{12} =$ Jacobian elements,

$$F(X(t), U(t), t) = \begin{bmatrix} f_1(X(t), U(t), t) \\ f_2(X(t), U(t), t) \end{bmatrix},$$

$$f_1(X(t), U(t), t): \quad \frac{dn(t)}{dt} = (\mu(s) - b)n(t)\left(1 - \frac{n(t)}{n_{max}}\right) + u_n(t),$$

$$f_2(X(t), U(t), t): \quad \frac{ds(t)}{dt} = -\frac{1}{Y}\mu(s)n(t) + u_s(t), \text{ and}$$

$$g(X(t), t): \quad v(t) = \left(k_{g1}\frac{1}{Y}\mu(s) + k_{g2}b\right)mn(t).$$

(2)

Here, the matrices that are coefficients of the vector of the state variables "$X(t)$" and the vector of the manipulated variables "$U(t)$" are partial derivative matrices evaluated by the equilibrium point of the Jacobian matrix. They are parameters which provide information relating to the characteristics of the anaerobic digestion process according to operating conditions.

Parameter-estimation system

First, we performed a Z-transformation on the state-space model, referring to the appendix for details (Eqs. 12–14), to obtain discrete input and output relational expressions (Eq. 3):

$$a_f(q)y(k) = B_f(q)U(k),$$

where: $a_f(q) = q^{-2} + (-a_{11} - a_{22})q^{-1} + (a_{11}a_{22} - a_{12}a_{21})$

$$= q^{-2} + a_1 q^{-1} + a_2,$$

and $B_f(q) = \begin{bmatrix} c_{11}(q^{-1} - a_{22}) + c_{12}a_{21} & c_{11}a_{12} + c_{12}(q^{-1} - a_{11}) \end{bmatrix}$

$$= \begin{bmatrix} b_1 q^{-1} + b_2 & b_3 q^{-1} + b_4 \end{bmatrix}.$$

(3)

The parameters of the original model (Eq. 2) were converted to "$a_{1,2}$" and "$b_{1,2,3,4}$". Once their values are estimated, biogas generation—"$y(k)$"—can be predicted by inputting the bacterial and substrate concentrations in the feedstock—"$U(k)$"—into Eq. 3. Next, we developed a control system using
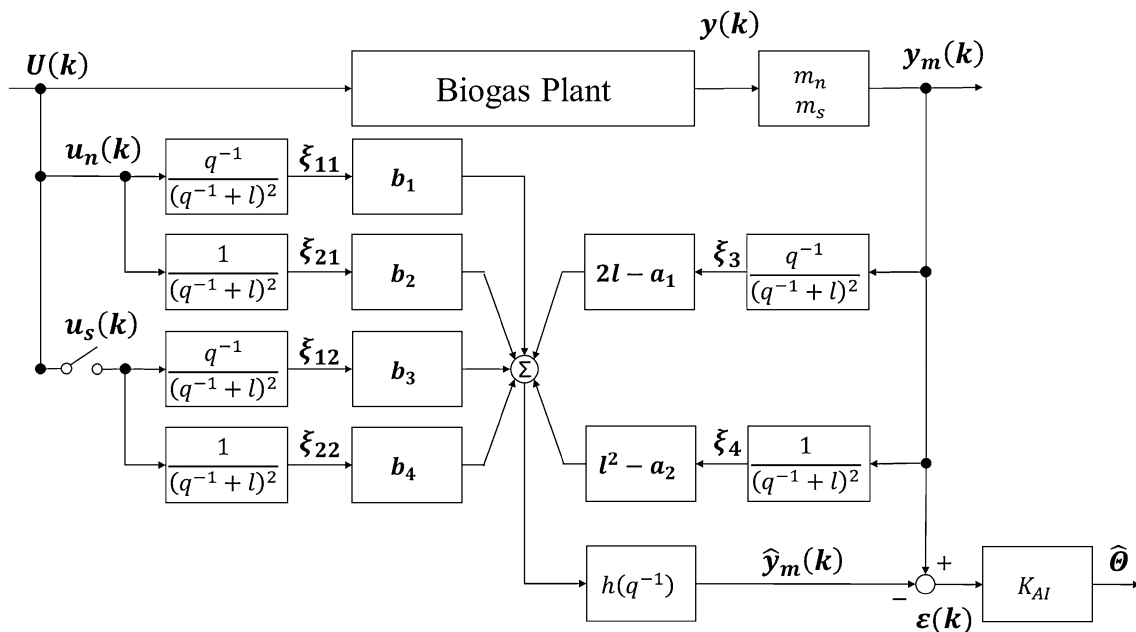
Fig. 3 Adaptive identifier. $U(k)$ feedstock input (kg/m^3/h), $u_n(t)$ bacteria input (kg/m^3/h), $u_s(t)$ substrate input (kg/m^3/h), $y(t)$ biogas flow rate (m^3/h), $y_m(t)$ scaled biogas flow rate (L/h), $\xi_{11,12,21,22,3,4}$ control signals, $a_{1,2}$" and "$b_{1,2,3,4}$ parameters, $h(q^{-1})$ is the filter, m_n scaling coefficient related to bacterial output, m_s scaling coefficient related to substrate output, l control system design constant, $\hat{y}_m(t)$ predicted scaled biogas flow rate (m^3/h), $\varepsilon(k)$ error (m^3/h), K_{AI} coefficient for least squares method, $\hat{\Theta}$ estimated parameters

the adaptive identification theory to estimate these parameters from actual operation data of the process [13]. The control system shown in Fig. 3 was denoted as the adaptive identifier. Input and output data were multiplied by the filter to provide the control signals "$\xi_{11,12,21,22,3,4}$" in the adaptive identifier. The control signals were multiplied by the operation parameters and integrated, and the linear relationship between the output and parameters with the proportionality constant as the control signal was derived using Eq. 4:

$$y(k) = h(q)\mathbf{\Theta}^{\mathrm{T}}\mathbf{\Xi}(k),$$

where : $\mathbf{\Theta} = \begin{bmatrix} b_1 & b_3 & b_2 & b_4 & 2l - a_1 & l^2 - a_2 \end{bmatrix}^{\mathrm{T}}$, and
$\mathbf{\Xi}(k) = \begin{bmatrix} \xi_{11}(k) & \xi_{12}(k) & \xi_{21}(k) & \xi_{22}(k) & \xi_3(k) & \xi_4(k) \end{bmatrix}\mathrm{T}.$
(4)

The parameters converted in Eq. 3 were further integrated into "Θ" in Eq. 4. If the values of this matrix element are obtained as described above, biogas generation can be predicted using Eq. 3. The difference between the measured output value and the value that was calculated using the estimated value of the parameter was defined as the output error "$\varepsilon(t)$" using Eq. 5:

$$\varepsilon(k) = y(k) - h(q)\hat{\mathbf{\Theta}}^{\mathrm{T}}\mathbf{\Xi}(k).$$
(5)

With the assumption that the estimated value of the parameter obtained with minimized error was a true value, the least squares method was applied to Eq. 5 with n data sets representing input and output. The least squares estimate of the parameter was obtained using the normal equation (Eq. 6):

$$\hat{\mathbf{\Theta}} = \left(\mathbf{\Xi}_n \mathbf{\Xi}_n^{\mathrm{T}} \right)^{-1} \mathbf{\Xi}_n \mathbf{Y}_n^{\mathrm{T}},$$

where: $\mathbf{\Xi}_n = \begin{bmatrix} \mathbf{\Xi}(1) & \mathbf{\Xi}(2) & \cdots & \mathbf{\Xi}(n) \end{bmatrix}^{\mathrm{T}}$, and (6)
$\mathbf{Y}_n = \begin{bmatrix} y(1) & y(2) & \cdots & y(n) \end{bmatrix}^{\mathrm{T}}.$

To quantitatively evaluate the prediction accuracy of the model with the estimated parameters, the goodness-of-fit index (GFI) was introduced (Eq. 7) [14]:

$$\mathrm{GFI} \begin{bmatrix} \% \end{bmatrix} = 100 \left(1 - \frac{y(k) - \hat{y}(k)}{y(k) - \mathrm{mean}(y)} \right).$$
(7)

The adaptive identifier includes a switch relating to substrate input because we consider anaerobic digestion process to be a 2-input and 1-output system. This enables the estimation of all parameters either with or without substrate input. The filter "$h(q^{-1})$", scaling coefficient "m_n and m_s" and control system design constant "l" were tuned so as to obtain the desired estimation result.
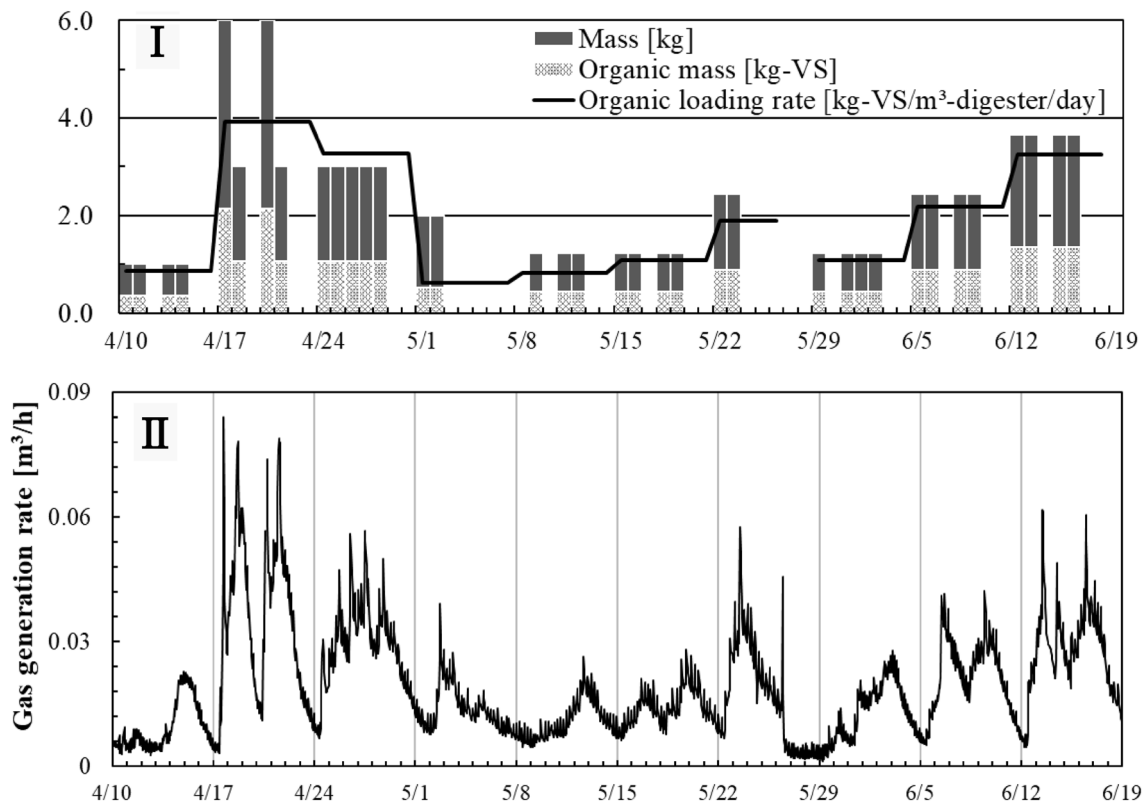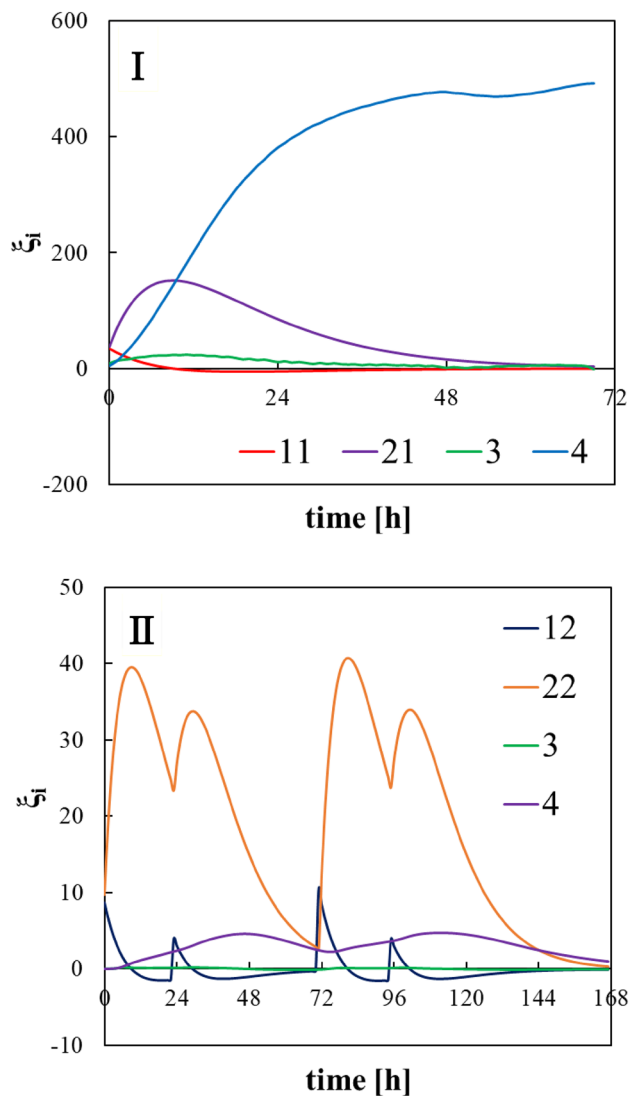

Fig. 4 Simulation data for (I) feedstock input and (II) gas generation rate

Table 1 Tuned constants

$h(q^{-1})$	m_n	m_s	l
1	1	0.001	0.1

$h(q^{-1})$ filter, m_n scaling coefficient related to bacterial output, m_s scaling coefficient related to substrate output, l control system design constant

Fig. 5 Control signals related to (I) bacterial input and (II) substrate input. Definitions: ξ_i is the controls signal. Numbers in the figure legend refer the subscripts of the control signals "i"

Simulation data

Substrate concentration was defined as the mass reduction that occurred following heating at 105 °C for 24 h then 600 °C for 3 h in an oven. Biogas generation was measured
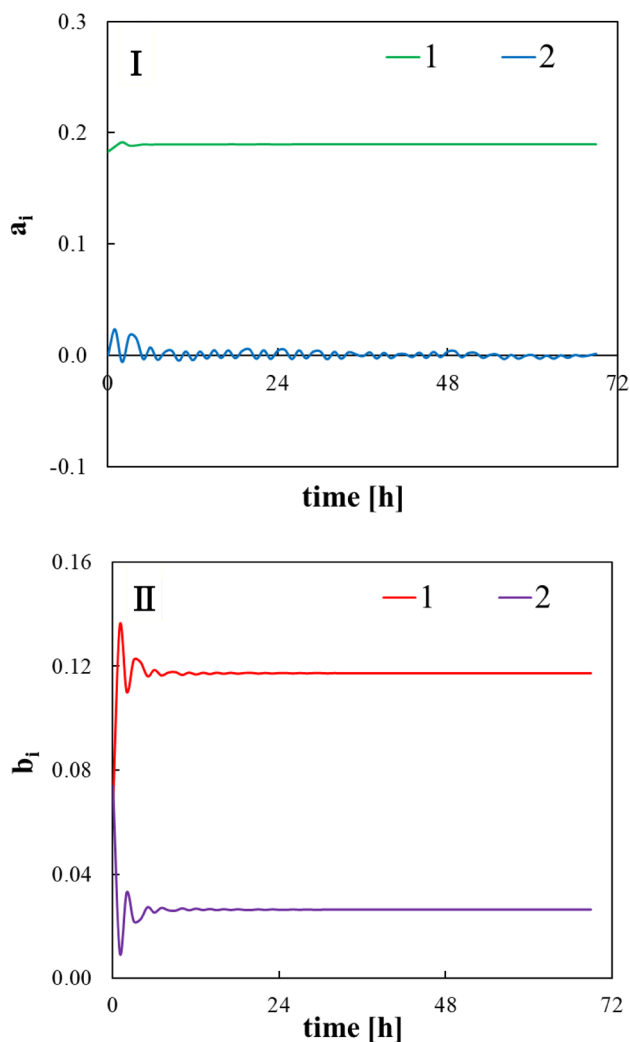
Fig. 6 Estimated parameters related to bacterial input for (I) the output side in (Eq. 3) and (II) the input side in (Eq. 3). Numbers in the figure legend refer the subscripts of the parameter "i". Definitions: a_i parameter on the output side in Eq. 3, b_i parameter on the output side in Eq. 3

hourly with a wet gas meter (W-NKDa-0.5B, SHINA-GAWA) and recorded using a data logger (Data mini LR 5000, HIOKI).

The data used in the simulation were the actual operation data collected in our laboratory in 2017 (Fig. 4). Bacterial input at 0 h was taken as the amount of substrate contained in the digestate at the beginning of the process, and feedstock input was performed four times at 0, 24, 72, and 96 h. Data of 3 days from 04/07/2017 (72 h data) when no feedstock was loaded and 1 week from 04/17/2017 (168 h data) when feedstock was loaded were used for model construction to estimate parameters. Data obtained during two 1-week periods from 06/05/2017 (168 h data) and 06/12/2017 (168 h data) were used for model validation. The organic loading rates of the model-construction period and
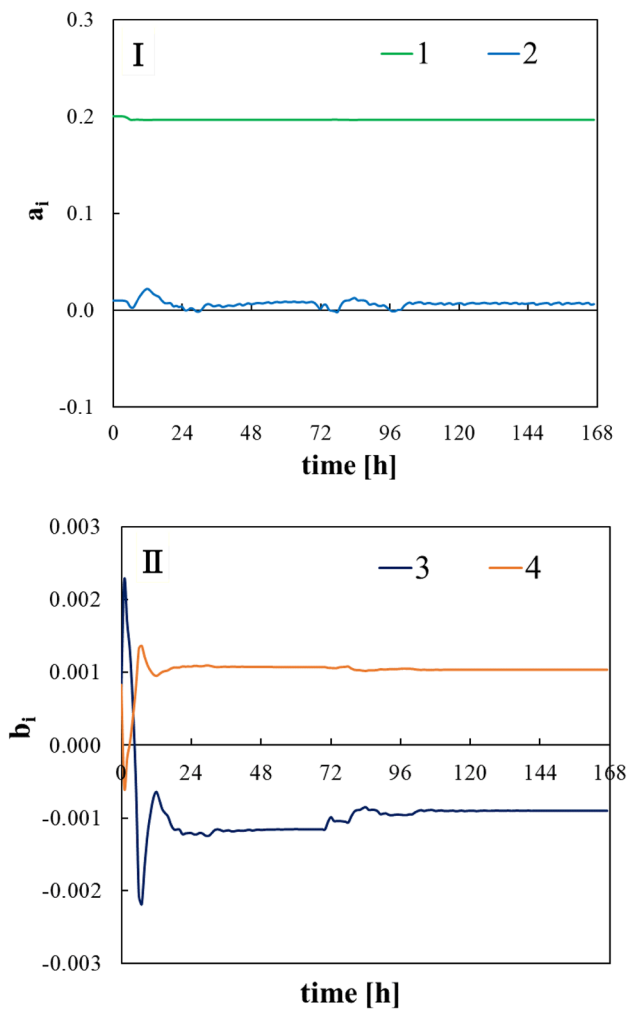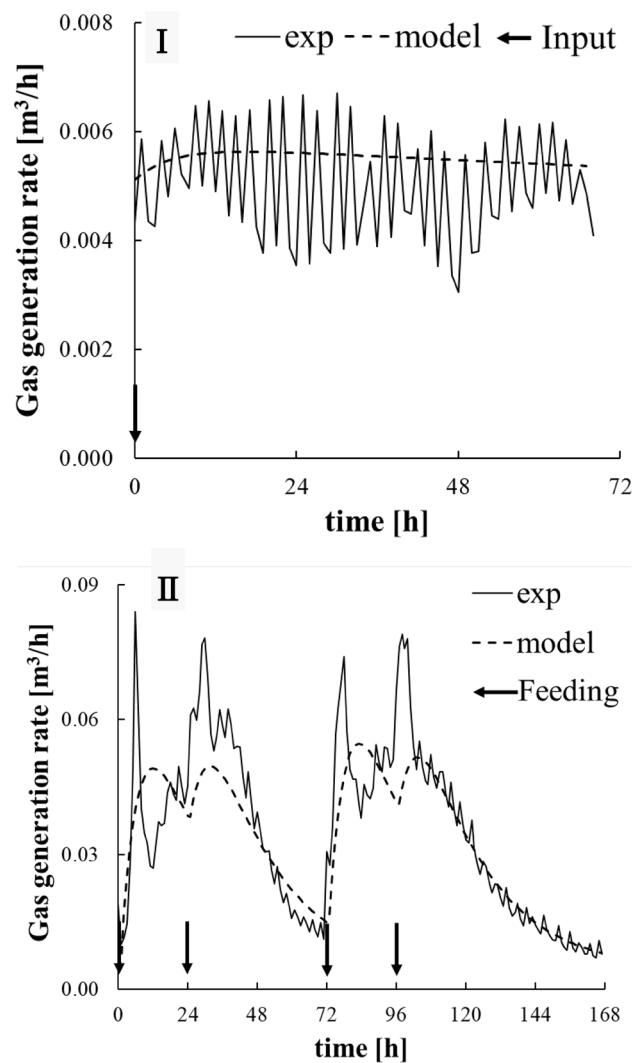
Fig. 7 Estimated parameters relating to substrate input on (I) the output side in (Eq. 3) and (II) the input side in (Eq. 3). Numbers in the figure legend refer the subscripts of the parameter "i". Definitions: a_i parameter on the output side in Eq. 3, b_i parameter on the output side in Eq. 3
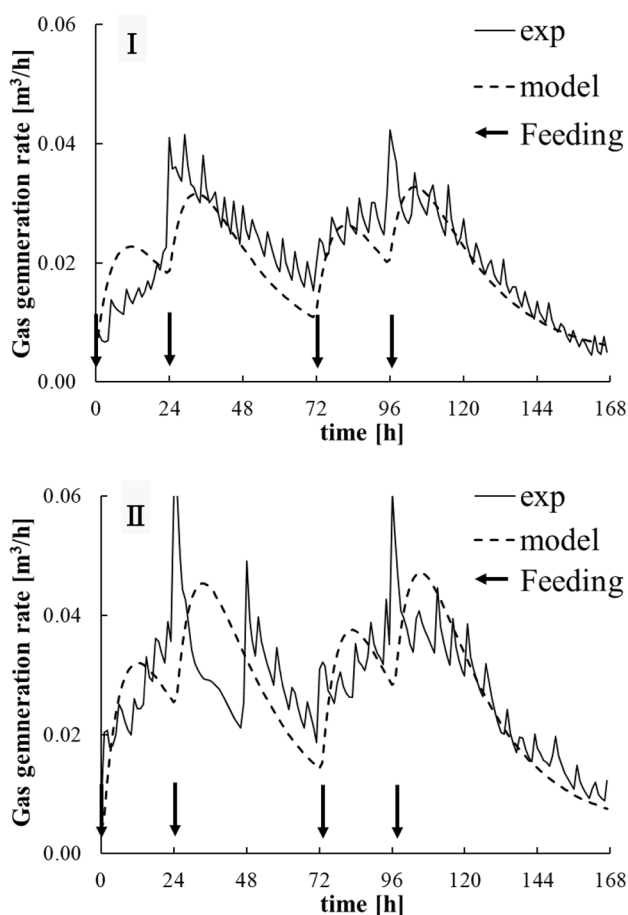

Fig. 8 Predicted gas generation for the data set that was used for model construction in relation to (I) bacterial input and (II) substrate input

the model-validation periods were different; the former was 3.96 (kg-VS/m³-digester/day) and the latter were 2.17 and 3.25 (kg-VS/m³-digester/day).

Results and discussion

The results of tuning the constants related to the control system are shown in Table 1. The control signals generated by the adaptive identifier are illustrated in Fig. 5. The bacterial and substrate inputs originally appear as several pulse signals because the anaerobic digestion processing flow used in this study was a semi-continuous system. As can be seen from Fig. 5, the pulse input is converted into a control signal that changes continuously according to the input. Figure 6 shows the results of parameter estimation using data from

the days where feedstock was not added. Although the estimated value of the parameter fluctuated largely at first, it gradually stabilized as the data increased, converging after about 24 h. This indicates that at least 24 h of identification experiment is required to estimate parameters related to bacterial input.
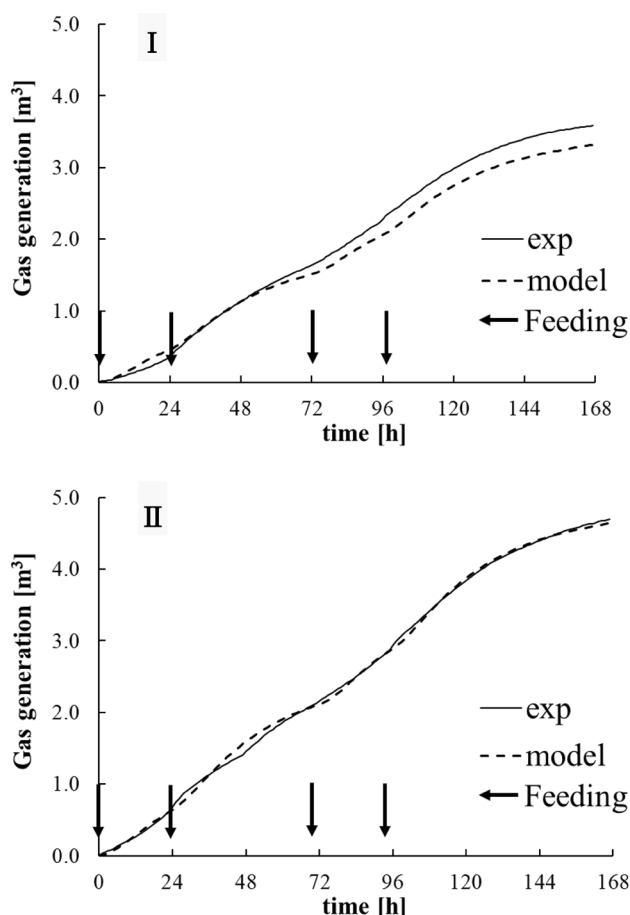
The parameter estimation results from data of the days when feedstock was loaded; in other words, the result of executing adaptive identification by turning on the switch relating to substrate input are shown in Fig. 7. The estimated value of the parameter changed greatly at the beginning of the experiment, converging after 120 h. Therefore, at least 120 h of identification experiment are necessary for the estimation of parameters related to substrate input.

Figure 8 shows the results of biogas generation prediction using a model constructed with the estimated parameters,

Fig. 9 Predicted gas generation for the data set that was used for model validation from the periods beginning (I) 06/05/2017 and (II) 06/12/2017

Fig. 10 Accumulated gas generation of the data set that was used for model validation from the periods beginning: (I) 06/05/2017 and (II) 06/12/2017

which reveal the high accuracy of the model. Figure 9 represents the results of validation performed with different data sets to those used for model construction. This was carried out to confirm the prediction accuracy of the model. The initial bacterial concentration of the model-construction period from 04/07/2017 to 04/17/2017 and the model-validation periods from 06/05/2017 to 06/12/2017 were different; the former values were 41 and 38 (kg/m^3) and the latter values were 33 and 34 (kg/m^3). The predicted biogas generation for the validation data sets exhibited low GFI (38.1% and 9.84%) because degassing due to agitation and heating had a significant influence on the recorded value for each hour. Therefore, a graph of accumulated biogas generation was constructed (Fig. 10). The GFIs for the two datasets are 84.39% and 96.53%. Figure 11 shows the GFI of accumulated biogas generation per day, which is more than 80%

even at the lowest value except for the values after the 4th day of the period from 06/05/2017, when biogas generation of the 3rd day could not be predicted. This indicates that the model and parameter-estimation system constructed in this study provide high prediction accuracy for periods of 1 day or more. By applying this model and parameter-estimation system, it is possible to predict the biogas generation of an anaerobic digestion process under various operating conditions. However, in an actual plant it is necessary to consider that operating conditions such as feedstock composition change continually. This issue could be overcome by introducing an oblivion factor that limits input data for the parameter-estimation system to, for example, only the last 72 h. Estimated parameters are thereby adaptively controlled in response to changes in operating conditions, enabling accurate prediction of biogas production.
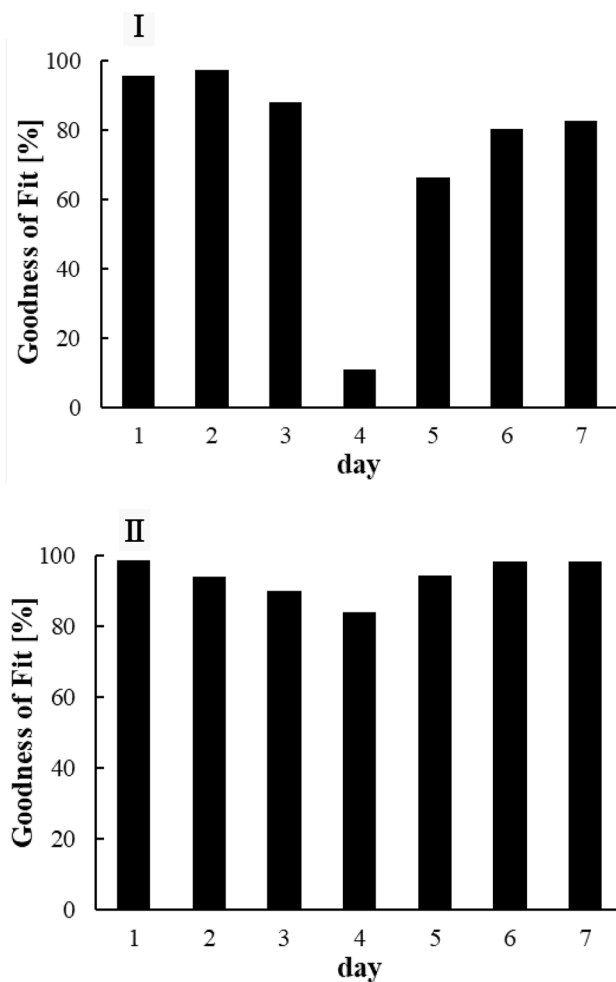
Fig. 11 Goodness-of-fit values per day of accumulated gas generation for the periods beginning: (I) 06/05/2017 and (II) 06/12/2017

Conclusions

In this study, which aimed to construct a biogas production management system that can be employed to stabilize renewable energy supplies, we established a model and parameter-estimation system which is applicable to anaerobic digestion processes with various operating conditions. The adaptive identifier control system can automatically estimate parameters from input and output data. Use of this adaptive identifier revealed that at least 24 and 120 h of identification experiments were required to converge the parameters with respect to bacterial and substrate inputs, respectively. The model and estimated parameters exhibit high prediction accuracy, and future developments should focus on constructing biogas production management systems that incorporate model predictive control of biogas generation. Such systems will enable the stabilization of renewable energy supplies.

Compliance with ethical standards

Appendix

Equation 2 was derived by the following procedure. First, the time evolution of state and output variables of a plant were considered as follows (Eq. 8):

$$\frac{\mathrm{d}X(t)}{\mathrm{d}t} = F(X(t), U(t), t)$$
$$y(t) = g(X(t), t). \tag{8}$$

Assuming a reaction near the equilibrium point, Eq. 8 became Eq. 9:

$$\frac{\mathrm{d}X(t)}{\mathrm{d}t} = F\big(X_{eq} + X'(t), U_{eq} + U'(t), t\big)$$
$$y(t) = g\big(X_{eq} + X'(t), t\big),$$
where $\big(X_{eq}, U_{eq}\big) = $ equilibrium point,
and $\big(X'(t), U'(t)\big) = $ perturbation. \tag{9}

The right side of Eq. 9 was rewritten by disregarding the second- and higher-order terms after Taylor expansion of a two-variable function (Eq. 10):

$$F\big(X_{eq} + X'(t), U_{eq} + U'(t), t\big) \approx F\big(X_{eq}, U_{eq}, t\big)$$
$$+ \left(X'(t)\frac{\partial}{\partial X(t)} + U'(t)\frac{\partial}{\partial U(t)}\right)F(X(t), U(t), t)\bigg|_{(X_{eq}, U_{eq}, t)}$$
$$y(t) = g\big(X_{eq}\big) + X'(t)\frac{\partial g}{\partial X(t)}\bigg|_{(X_{eq}, t)} \tag{10}$$

Finally, Eq. 2 was given by transporting the equilibrium point of Eq. 10 to the origin (Eq. 11):

$$\frac{\mathrm{d}X(t)}{\mathrm{d}t} = \frac{\partial F}{\partial X(t)}\bigg|_{(X_{eq}, U_{eq}, t)} X(t) + \frac{\partial F}{\partial U(t)}\bigg|_{(X_{eq}, U_{eq}, t)} U(t)$$
$$y(t) = \frac{\partial g}{\partial X(t)}\bigg|_{(X_{eq}, U_{eq}, t)} X(t). \tag{11}$$

Equation 3 was derived by Z-transformation of the state-space model (Eq. 2). This is equivalent to Laplace transform on discrete time, and it replaces the operator in the Laplace

transform with a delay operator. The Z-transformation of Eq. 2 is represented by Eq. 12:

$$q^{-1}X(k) - X(0) = A_p X(t) + B_p U(t)$$
$$y(k) = C_p X(k), \tag{12}$$

where q^{-1} = delay operator.

Since the coefficient of the first variable on the left side of Eq. 12 is arithmetically scalar, Eq. 13 was obtained from Eq. 12:

$$X(k) = \left(q^{-1}I - A_p\right)^{-1}\left(B_p U(t) + X(0)\right)$$
$$y(k) = C_p X(k). \tag{13}$$

Here, we did not consider the initial value in this study. Equation 3 was finally given by combining the two expressions of Eq. 13, as follows:

$$y(k) = C_p\left(q^{-1}I - A_p\right)^{-1}B_p U(t),$$
$$\text{where: } \left(q^{-1}I - A_p\right)^{-1} = \frac{\text{adj}\left(q^{-1}I - A_p\right)}{\det\left(q^{-1}I - A_p\right)}$$
$$= \frac{1}{q^{-2} + \left(-a_{11} - a_{22}\right)q^{-1} + \left(a_{11}a_{22} - a_{12}a_{21}\right)}$$
$$\times \begin{bmatrix} q^{-1} - a_{22} & a_{12} \\ a_{21} & q^{-1} - a_{11} \end{bmatrix}. \tag{14}$$

To verify the mechanism of the adaptive identifier shown in Fig. 3, we obtained the expansion of Eq. 4, as follows:

$$y(k) = h(q)\big(b_1\xi_{11}(k) + b_3\xi_{12}(k) + b_2\xi_{21}(k)$$
$$+ b_4\xi_{22}(k) + \left(2l - a_1\right)\xi_3(k) + \left(l^2 - a_2\right)\xi_4(k)\big)$$
$$= h(q)\bigg(b_1\frac{q^{-1}}{(q^{-1} + l)^2}u_n(k) + b_3\frac{1}{(q^{-1} + l)^2}u_n(k)$$
$$+ b_2\frac{q^{-1}}{(q^{-1} + l)^2}u_s(k) + b_4\frac{1}{(q^{-1} + l)^2}u_s(k)$$
$$+ \left(2l - a_1\right)\frac{q^{-1}}{(q^{-1} + l)^2}y(k) + \left(l^2 - a_2\right)\frac{1}{(q^{-1} + l)^2}y(k)\bigg)$$
$$= h(q)\bigg(\frac{b_1 q^{-1} + b_3}{(q^{-1} + l)^2}u_n(k) + \frac{b_2 q^{-1} + b_4}{(q^{-1} + l)^2}u_s(k)$$
$$+ \frac{2q^{-1}l - a_1 q^{-1} + l^2 - a_2}{(q^{-1} + l)^2}y(k)\bigg). \tag{15}$$

Furthermore, organizing Eq. 15:

$$\left(\left(q^{-1} + l\right)^2 - \left(2q^{-1}l - a_1 q^{-1} + l^2 - a_2\right)\right)y(k)$$
$$= h(q)\left(\left(b_1 q^{-1} + b_3\right)u_n(k) + \left(b_2 q^{-1} + b_4\right)u_s(k)\right). \tag{16}$$

It can be said that this equation and Eq. 3 are identical. Therefore, the linear relationship between the output and parameters (Eq. 4) was derived from Eq. 3 and gave reliable estimation results.

References

1. Noike T (2009) Anaerobic digestion. Tokyo, Gihodo, p 283
2. Ghosh S, Conrad JR, Klass DL (1975) Anaerobic acidogenesis of wastewater sludge. J Water Pollut Control Feder 47:30–45
3. Mendez-Acosta HO, Palacios-Ruiz B, Alcaraz-Gonzalez V, Gonzalez-Alvarez V, Garcia-Sandoval JP (2016) A robust control scheme to improve the stability of anaerobic digestion processes. J Process Control 20:375–383
4. Mauky E, Weinrich S, Nagele HJ, Jacobi HF, Liebetran J, Nelles M (2016) Model predictive control for demand-driven biogas production in full scale. Chem Eng Technol 39:652–664
5. Batstone D, Keller J, Angelidaki I, Kalyuzhnyi S, Pavlostathis S, Rozzi A, Sanders WT, Siegrist H, Vavilin VA (2002) The IWA anaerobic digestion model no. 1. Water Sci Technol 45:65–73
6. IEA BIOENERGY (2001) Biogas and more!: Systems and markets overview of anaerobic digestion. AEA Technol. Environ, Oxfordshire
7. Hend M, Hatem K (2015) Regulation of biogas production through waste water anaerobic digestion process modeling and parameters optimization. Waste Biomass Valoriz 6:29–35
8. Lauterbök B, Ortner M, Haider R, Fuchs W (2012) Counteracting ammonia inhibition in anaerobic digestion by removal with a hollow fiber membrane contactor. Water Res 46:4861–4869
9. Nakajima S, Shimizu N, Ishiwata H, Ito T (2016) The start-up of thermophilic anaerobic digestion of municipal solid waste. J Jpn Inst Energy 95:645–647
10. Charles JB, Sonia H (2013) Optimisation of biogas yields from anaerobic digestion by feedstock type. In: By Wellinger A, Murphy J, Baxter D (eds) The biogas handbook. Woodhead Publishing Limited, Cambridge, pp 131–161
11. Robert MM (1976) Simple mathematical models with very complicated dynamics. Nature 261:459–467
12. Nagatani M (1973) Reaction rate of microorganisms. J Brew Soc Jpn 68:829–834
13. Byrme RH, Abdallah CT (1995) Design of a model reference adaptive controller for vehicle road following. Math Comput Modell 22:343–354
14. Mulaik SA, James LR, Van Alstine J, Bennett N, Lind S, Stilwell CD (1989) Evaluation of goodness-of-fit indices for structural equation models. Psychol Bull 105:430–445